ChemComm

Accepted Manuscript

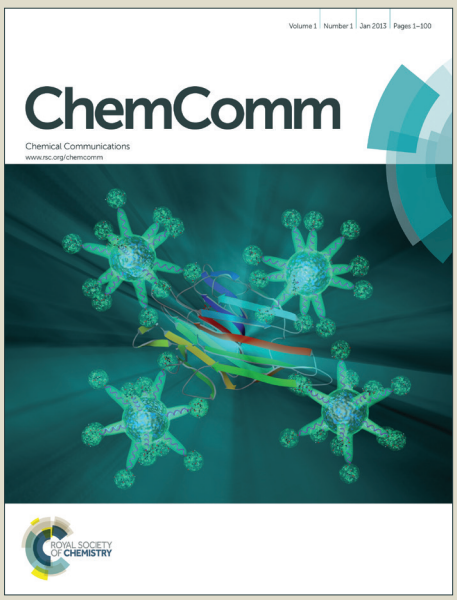

ROYAL SOCIETY OF CHEMISTRY

www.rsc.org/chemcomm

Journal Name

RSCPublishing

COMMUNICATION

Cu^{1+} in HKUST-1: Selective gas adsorption in the presence of water

Cite this: DOI: 10.1039/xoxxoooooox

Received ooth January 2012,
Accepted ooth January 2012

DOI: 10.1039/xoxxoooooox

www.rsc.org/

Nour Nijem,[a] Hendrik Bluhm,[b] May L. Ng,[b,d] Martin Kunz,[b] Stephen R. Leone,[a,c] and Mary K. Gilles [b]

[a]Departments of Chemistry and Physics, University of California Berkeley, CA 94720
[b]Advanced Light Source, Lawrence Berkeley National Lab, 1-Cyclotron Rd, Berkeley, CA 94720
[c]Chemical Sciences Division, Lawrence Berkeley National Lab, 1-Cyclotron Rd, CA 94720
[d]SUNCAT Center for Interface Science and Catalysis, SLAC National Accelerator Laboratory, Menlo Park, CA 94025

Spectroscopic evidence for an enhanced binding of Nitric Oxide (NO) to metal centers with lower oxidation (open Cu^{1+} sites) in $Cu_3(btc)_2$ (HKUST-1) is presented. The Cu^{1+} sites created by thermal treatment or X-ray exposure exhibit a preferential adsorption of NO compared to H_2O. This phenomenon demonstrates the potential use of MOFs with lower oxidation metal centers for selective gas separation.

Gas separation technologies, in particular distillation, account for the majority of industrial energy use. Adsorptive separation by porous materials is an alternative green separation method that requires less energy and produces fewer by-products. Adsorptive separation exploits differences in gas adsorption propensities of the adsorbent either by kinetic diffusivity, or molecular sieving and thermodynamic equilibrium effects.[1, 2] Currently, porous metal organic frameworks (MOFs) are the focus of numerous research efforts in this area.[2-4] MOFs, also known as porous coordination polymers, are composed of a metal center (or polynuclear metal clusters) linked through organic components by coordination bonds to form crystalline structures.[5, 6] Their high specific surface areas and tuneable structures, containing various chemical functionalities, make them attractive in many areas, from gas adsorption and separation to catalysis, sensing, electron conductivity, and biomedical applications.[2, 7-10] Major obstacles to the application of MOFs for gas separation are their structural instability in the presence of water (a major component of flue gas),[11, 12] and the higher preferential adsorption of water on open metal sites[13,14] compared to other gases. Methods to overcome these barriers have focused on the use of perflourinated linkers and the inclusion of protective groups.[15-20]

MOFs with unsaturated metal centers such as CPO-27 and $Cu_3(btc)_2$ (also known as HKUST-1 and where btc = 1,3,5 benzenetricarboxylate) have been considered for gas separation and storage because of the strong interaction of gases with the open metal sites.[21-23] A drawback in their use for gas separation is the stronger binding of H_2O to open metal centers compared to the gas being separated. For example, in the case of $Cu_3(btc)_2$, the binding energy is ~47.3 kJ/mol for H_2O compared to ~29.8 kJ/mol for CO_2.[24, 25] $Cu_3(btc)_2$ was selected as a model system to study the influence of the metal center's oxidation state on its adsorptive interactions. $Cu_3(btc)_2$ is composed of Cu^{2+} paddle wheel type nodes (Cu^{2+}-dimers) connected by 1,3,5-benzenetricarboxylate linkers forming large interconnecting channels surrounded by small tetrahedral pockets.[26] The unsaturated metal centers in $Cu_3(btc)_2$ make it attractive for gas adsorption, separation, and catalysis.[2, 25, 27-29] Enhancing the binding of gases such as CO_2, NO, and SO_2 compared to water, is crucial for gas separation applications of MOFs. Here, we present the first evidence for an enhanced interaction of NO (compared to water) with Cu^{1+} sites in the $Cu_3(btc)_2$ framework. Reduction of Cu^{2+} in $Cu_3(btc)_2$ occurs under thermal treatment or X-ray irradiation.[30-32] Formation of Cu^{1+} defects in $Cu_3(btc)_2$ were correlated with activation temperatures (removal of solvent from the pores by heating) and were created by a missing linker.[30, 31] To experimentally simulate controllable Cu^{2+} reduction, we use soft X-rays both to probe and reduce the metal centers. X-ray beam induced effects are well known and have been observed in self-assembled monolayers and biological materials.[35,50] Photo-reduction of Cu^{2+} in copper acetate results from the interaction of Auger and low energy electrons (<50 eV) with the material.[32] X-ray exposure promotes reduction of the Cu^{2+} in HKUST-1, similar to reduction caused by sample anneal (activation) temperatures (Figure S1).[30] Near Edge X-ray Absorption Fine Structure (NEXAFS) spectra of the Cu L-edge from $Cu_3(btc)_2$ thin films exhibit a controlled X-ray photo-reduction of the Cu^{2+} metal centers as a function of X-ray exposure. Approximately 4% of the Cu in the pristine sample was Cu^{1+} and this increased to ~12% with X-ray irradiation for 12 minutes (photon flux $1.5x10^{12}$ photon/second, beam size of 0.2x0.1 mm^2). Changes in the copper oxidation state observed in the Cu L-edge (NEXAFS) spectra from soft X-ray

irradiation are consistent with those observed when activating the sample at 180 °C (section 1 of supporting information).

Previously, spectroscopic techniques such as IR and Raman spectroscopies, nuclear magnetic resonance and pair distribution functions from X-ray diffraction have provided a mechanistic understanding of gas adsorption in MOFs.[15, 23, 33-39] In this work, we use ambient pressure photoelectron spectroscopy (APPES) to investigate chemical interactions occurring during initial gas adsorption. Homogeneous $Cu_3(btc)_2$ thin films were synthesized following the layer-by-layer method (XRD and film growth are shown in Figure S4).[40,41-44] NO adsorption isotherms, derived from gas phase quartz crystal microbalance (QCM) measurements are consistent with values reported for the powder $Cu_3(btc)_2$ framework, ~3.3 mmol/g at 700 Torr (Figure S5).[29]

The interaction of NO with $Cu_3(btc)_2$ is examined with photoelectron and NEXAFS spectra. The upper panel of Figure 1 shows N 1s X-ray Photoelectron spectra (XPS) as a function of NO pressure (0.03-0.2 Torr, 4 min X-ray exposure time for each spectrum). The two sharp gas phase NO features (filled grey areas) appear ~8 eV lower than the free gas phase due to charging of the substrate affecting the gas in its vicinity. In addition, two distinct nitrogen species are observed in the N 1s region at 403.5 and 406 eV. These peak intensities increase with increasing NO pressure.[45] The 403.5 eV N 1s peak is assigned to neutral adsorbed NO, while the higher binding energy peak (406 eV) is assigned to adsorbed NO^+.[46] In a very simplistic initial state model, the binding energy peak positions are related to how strongly electrons are bound to the nucleus. Removal of an electron from the nitrogen results in a stronger attraction of the remaining electrons to the nucleus, therefore increasing the binding energy of the N 1s electron. In general, the core electron experiences a change in chemical environment when a change in potential (charge distribution) of a valence shell occurs

The effect of NO adsorption on the copper oxidation state is apparent in the NEXAFS spectra (Figure 1, bottom). Bottom part of Figure 1 shows the Cu L-edge NEXAFS spectra measured under ultra high vacuum (UHV), 0.01 and 0.1 Torr of NO. Normalizing the spectra to the pre-edge intensity eliminates contributions from other elements to the background. NEXAFS spectra measured in UHV (Figure 1, top) show contributions from both Cu^{2+} and Cu^{1+}.[47, 48]The intensity of the Cu^{1+} peak decreases as NO is introduced and a corresponding increase in the area under the Cu^{2+} peak is observed. This indicates oxidation of the Cu^{1+} by NO to form Cu^{2+} centers that are different in nature than the pristine Cu^{2+} in HKUST-1. (Figure S2). The contribution of both Cu species is determined from the area under the Cu 2p photoelectron peaks measured at UHV (Figure S2). Consistent with previous reports, Cu^{1+} atoms were estimated to be ~4±1% of the total Cu species.[30]

Assignment of the NO species to specific adsorption sites was performed by varying the X-ray exposure time on the X-ray photoemission N 1s spectra (inset of top panel of Figure 1). The inset in the top part of Figure 1 shows the 403.5 and 406 eV N 1s peak integrated area as a function of beam exposure time. Varying beam exposure time serves as a method to control the formation of X-ray photo-reduced Cu^{1+} (details in section S1 of SI). Controlled X-ray exposure in the presence of NO promotes adsorption of NO at newly formed Cu^{1+} sites. At low X-ray exposures a single peak at 403.5 eV is observed. The 406 eV peak appears only after an increased X-ray exposure time (further details in section 4 of supporting information). Therefore, the 403.5 eV peak is assigned to NO adsorbed at the Cu^{2+}, and the 406 eV peak to NO adsorbed at newly formed Cu^{1+}. The chemical integrity and crystallinity of the framework (post X-ray exposure) was verified by examining the C 1s and O 1s XPS spectra and X-ray diffraction patterns (SI section S4).

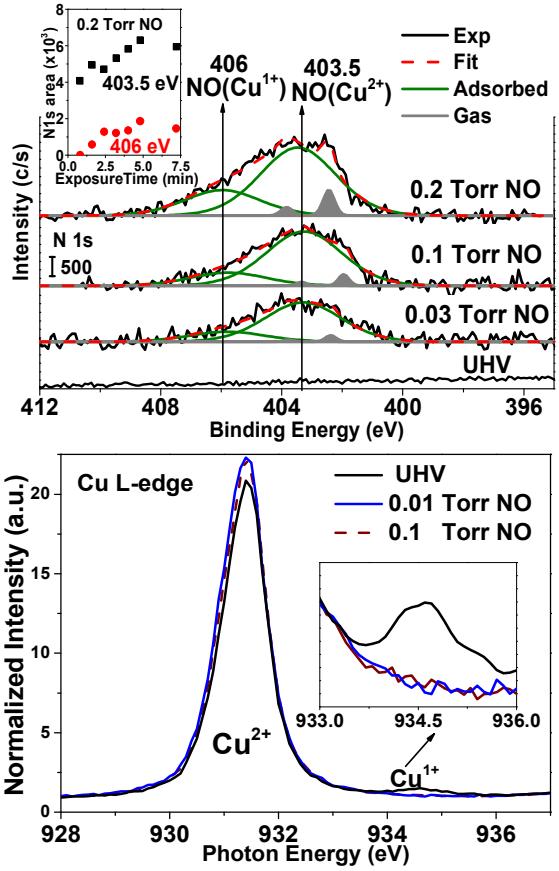

Fig. 1 Top: X-ray photoelectron spectra of N 1s at UHV and as a function of NO pressure. Peaks at 403.5 and 406 eV arise from adsorption of NO at Cu^{2+} and Cu^{1+} sites respectively. The sharp (grey) spectral features arise from gas phase NO. X-ray photoelectron spectra are collected with 600 eV incident photon energies. Inset shows the N 1s peak integrated areas as a function of beam exposure time. Bottom: Cu L-edge NEXAFS spectra in UHV and as a function of NO pressure.

XPS peak intensities are directly correlated to the amount of a specific species present; therefore the amounts of NO adsorbed at each site are quantitative. Initially, nitrogen accounts for ~3.4±0.2% of the total atomic percentage of species (C 1s, Cu 2p, O 1s, N 1s). With an X-ray exposure of 432 seconds (4.2 minutes), the total nitrogen contribution increases to ~6±0.3% (inset, top panel Figure 1). Of the total N 1s peak area, ~55±5% corresponds to NO adsorbed at the initial Cu^{2+} sites, ~25±3% corresponds to newly occupied Cu^{2+} of the Cu^{2+}-Cu^{1+} dimers, and ~20±2% of the total integrated area corresponds to NO adsorbed at new Cu^{1+} sites. The increase in the area under the N 1s peak (403.5 eV) associated with NO adsorbed at the Cu^{2+} suggests that initially occupied Cu^{2+} sites are not transformed, rather the unoccupied Cu^{2+}centers are reduced to Cu^{1+}, providing new adsorption sites. The new Cu^{2+} sites in the Cu^{2+}-Cu^{1+} dimers are occupied only after formation of Cu^{1+}; therefore, at the same pressure we expect the binding strength to the newly formed sites to be equivalent to or higher than NO adsorbed at the original Cu^{2+}-Cu^{2+} dimers.

To examine the preferential adsorption of NO at the Cu^{2+} and Cu^{1+} sites in the presence of water, N 1s spectra of pre-adsorbed NO are recorded as a function of partial pressure of water vapor (Figure 2). The top panel of Figure 2 shows N 1s XPS spectra recorded with 0.05 Torr of NO, then after addition of H_2O at 1:1 NO:H_2O, and with 1:10 NO:H_2O partial pressure ratios. The bottom panel summarizes the normalized integrated areas of each of the adsorbed species as a function of H_2O partial pressure (normalization of the integrated area to the C 1s signal facilitates comparison of spectra collected at different sample locations). A dramatic decrease (~71%) in the normalized integrated area of the 403.5 eV peak (Figure 2, bottom) with increasing partial pressure of water indicates that NO is replaced by water at the Cu^{2+} sites. On the contrary, the normalized integrated area of NO adsorbed at Cu^{1+} (406 eV) remains relatively constant regardless of H_2O partial pressure (Figure 2). In the presence of ten times more water than NO, NO is almost completely removed from Cu^{2+} but still adsorbs at Cu^{1+} (Figure 2, top). This clearly indicates that Cu^{1+} sites (potentially formed by X-ray exposure or temperature) selectively adsorb NO in the presence of water, i.e. Cu^{1+} has a higher binding strength for NO as compared to H_2O (Figure 2).

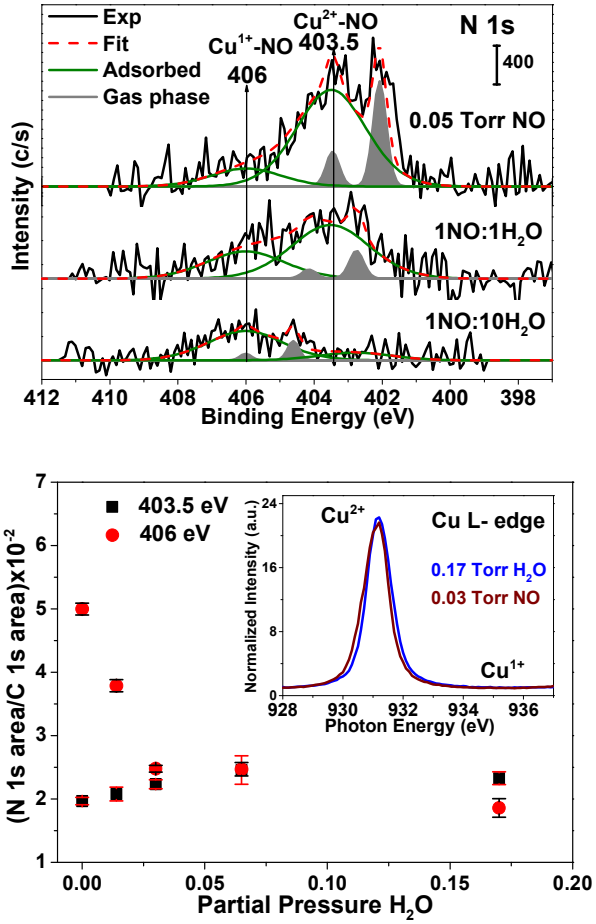

Fig. 2 Top panel: N 1s X-ray photoelectron spectra of $Cu_3(btc)_2$ at a fixed pressure of 0.05 Torr NO (top) with increasing H_2O pressure (middle 1:1 NO:H_2O and lower 1:10 NO:H_2O) Bottom panel: normalized integrated area of N 1s peaks to C 1s as a function of partial pressure of H_2O. N 1s spectra are collected with 600 eV incident photon energies. Inset shows Cu L-edge NEXAFS spectra for 0.03 Torr NO (wine) and after addition of 0.17 Torr H_2O (blue). Error in estimation of the ratio was found to be between 10^{-3} to $5x10^{-4}$.

At the highest H_2O partial pressures, the integrated area of the remaining 403.5 eV peak represents the contribution from adsorbed NO that is not replaced by water or NO adsorbed at Cu^{2+} sites of the newly created Cu^{1+}-Cu^{2+} dimers with a lower affinity to water. Primarily due to replacement of NO by water at Cu^{2+}-Cu^{2+} dimers the overall NO capacity deceases by ~50%. NEXAFS spectra taken upon exposure to H_2O show no change in the copper oxidation state, indicating that NO remains adsorbed at the Cu^{1+} (inset bottom panel Figure 2). O 1s XPS spectra confirm the presence of adsorbed water (peak at 534 eV) replacing the pre-adsorbed NO at the Cu^{2+} sites (Figure S12).

To understand the differences in binding strength of NO to Cu^{2+} and Cu^{1+} it is beneficial to examine the interactions involved. For the case of NO adsorbed on Cu^{2+}, the bonding is dominated by a σ donation with a π back-donation.[25, 29] The findings presented in this work show that for NO adsorbed at the Cu^{1+}, a stronger interaction exists. The higher binding energy position of the N 1s peak (406 eV) (associated with NO adsorbed at Cu^{1+}) and the oxidation of the Cu^{1+} (Figure 1, bottom) by the NO points towards the likelihood of a π back-donation from the Cu^{1+} 3d orbital to the NO, with an additional covalent donation from NO and Cu^{1+} electrons to the bonding region.[49] π back-donation bonding in the latter case is similar to bonding of CO to Cu^{1+} having a stronger binding energy than σ donation.[30]

Conclusions

In Summary, we present experimental evidence that open metal centers with reduced oxidation state (Cu^{1+}) in MOFs interact more strongly with adsorbed gases, such as nitric oxide, than metal centers with a higher oxidation state (Cu^{2+}). In particular, we probe interactions of NO in the presence of water with Cu^{2+} and Cu^{1+} (reduced Cu^{2+}) metal centers in $Cu_3(btc)_2$. These reduced sites can be created during thermal activation or photo-reduction. When produced via controlled photo-reduction, X-ray photoemission spectroscopy elucidates the nature of the chemical interactions involved. The photo-reduced Cu^{1+} sites in $Cu_3(btc)_2$ demonstrate a higher affinity for NO compared to water, with a stronger binding strength than on Cu^{2+}. This phenomenon is of broad interest because it demonstrates the potential use of frameworks with metal centers of reduced oxidation for gas separation, having enhanced interactions with the gas being separated and a smaller affinity for water.

Notes and references

[a] Departments of Chemistry and Physics, University of California Berkeley, CA 94720
[b] Advanced Light Source, Lawrence Berkeley National Lab, 1-Cyclotron Rd, Berkeley, CA 94720
[c] Chemical Sciences Division, Lawrence Berkeley National Lab, 1-Cyclotron Rd, CA 94720

† Electronic Supplementary Information (ESI) available: Supporting information for experimental methods, nitric oxide adsorption isotherm, sample treatment and beam induced effects, assignment of NO adsorbed species, thermal stability of NO adsorbed species and influence of water on NO adsorbed species. See DOI: 10.1039/c000000x/

This work was supported by the Laboratory Directed Research and Development at Lawrence Berkeley National Laboratory; the Advanced Light Source (ALS) is supported by the U.S. Department of Energy, Office of Science, Office of Basic Energy Sciences, Chemical Sciences, Geosciences and Biosciences Division at Lawrence Berkeley National Laboratory under Contract No. DE-AC02-05CH11231. M. K. G., H. B., and beamline 11.0.2 at the ALS are supported through the Condensed

Phase and Interfacial Molecular Science Program of DOE. The microdiffraction program at the ALS on BL 12.3.2 was made possible by NSF Grant No. 0416243. N. N. and S. R. L. were supported by the Office of the Secretary of Defense National Security Science and Engineering Faculty Fellowship.

1. J.-R. Li, R. J. Kuppler and H.-C. Zhou, *Chem. Soc. Rev.*, 2009, **38**, 1477-1504.
2. K. Sumida, D. L. Rogow, J. A. Mason, T. M. McDonald, E. D. Bloch, Z. R. Herm, T.-H. Bae and J. R. Long, *Chem. Rev.*, 2011, **112**, 724-781.
3. Z. Zhang, Y. Zhao, Q. Gong, Z. Li and J. Li, *Chem. Commun.*, 2013, **49**, 653-661.
4. J.-R. Li, J. Sculley and H.-C. Zhou, *Chem. Rev.*, 2011, **112**, 869-932.
5. M. O'Keeffe and O. M. Yaghi, *Chem. Rev.*, 2011, **112**, 675-702.
6. N. Stock and S. Biswas, *Chem. Rev.*, 2011, **112**, 933-969.
7. R. J. Kuppler, D. J. Timmons, Q.-R. Fang, J.-R. Li, T. A. Makal, M. D. Young, D. Yuan, D. Zhao, W. Zhuang and H.-C. Zhou, *Coord. Chem. Rev.*, 2009, **253**, 3042-3066.
8. O. K. Farha, A. Özgür Yazaydın, I. Eryazici, C. D. Malliakas, B. G. Hauser, M. G. Kanatzidis, S. T. Nguyen, R. Q. Snurr and J. T. Hupp, *Nat. Chem.*, 2010, **2**, 944-948.
9. J. Lee, O. K. Farha, J. Roberts, K. A. Scheidt, S. T. Nguyen and J. T. Hupp, *Chem. Soc. Rev.*, 2009, **38**, 1450-1459.
10. N. C. Jeong, B. Samanta, C. Y. Lee, O. K. Farha and J. T. Hupp, *J. Am. Chem. Soc.*, 2011, **134**, 51-54.
11. J. B. DeCoste, G. W. Peterson, H. Jasuja, T. G. Glover, Y.-G. Huang and K. S. Walton, *J. Mater. Chem. A*, 2013, **1**, 5642-5650.
12. K. Tan, N. Nijem, P. Canepa, Q. Gong, J. Li, T. Thonhauser and Y. J. Chabal, *Chem. Mater.*, 2012, **24**, 3153-3167.
13. P. Canepa, N. Nijem, Y. J. Chabal and T. Thonhauser, *Phys. Rev. Lett.*, 2013, **110**, 026102.
14. J. B. DeCoste, G. W. Peterson, B. J. Schindler, K. L. Killops, M. A. Browe and J. J. Mahle, *J. Mater. Chem. A*, 2013, **1**, 11922-11932.
15. N. Nijem, P. Canepa, U. Kaipa, K. Tan, K. Roodenko, S. Tekarli, J. Halbert, I. W. H. Oswald, R. K. Arvapally, C. Yang, T. Thonhauser, M. A. Omary and Y. J. Chabal, *J. Am. Chem. Soc.*, 2013, **135**, 12615-12626.
16. H. Jasuja, Y.-G. Huang and K. S. Walton, *Langmuir*, 2012, **28**, 16874-16880.
17. N. Planas, A. L. Dzubak, R. Poloni, L.-C. Lin, A. McManus, T. M. McDonald, J. B. Neaton, J. R. Long, B. Smit and L. Gagliardi, *J. Am. Chem. Soc.*, 2013, **135**, 7402-7405.
18. C. Yang, X. Wang and M. A. Omary, *J. Am. Chem. Soc.*, 2007, **129**, 15454-15455.
19. A. Das, P. D. Southon, M. Zhao, C. J. Kepert, A. T. Harris and D. M. D'Alessandro, *Dalt. Trans.*, 2012, **41**, 11739-11744.
20. B. Weinberger, D. L. Laskin, D. E. Heck and J. D. Laskin, *Toxicol. Sci.*, 2001, **59**, 5-16.
21. J. L. C. Rowsell and O. M. Yaghi, *J. Am. Chem. Soc.*, 2006, **128**, 1304-1315.
22. A. C. McKinlay, B. Xiao, D. S. Wragg, P. S. Wheatley, I. L. Megson and R. E. Morris, *J. Am. Chem. Soc.*, 2008, **130**, 10440-10444.
23. P. D. C. Dietzel, R. E. Johnsen, H. Fjellvag, S. Bordiga, E. Groppo, S. Chavan and R. Blom, *Chem. Commun.*, 2008, 5125-5127.
24. C. R. Wade and M. Dinca, *Dalt. Trans.*, 2012, **41**, 7931-7938.
25. T. Watanabe and D. S. Sholl, *J. Chem. Phys.*, 2010, **133**, 094509.
26. S. S.-Y. Chui, S. M.-F. Lo, J. P. H. Charmant, A. G. Orpen and I. D. Williams, *Science*, 1999, **283**, 1148-1150.
27. E. Pérez-Mayoral and J. Čejka, *Chem. Cat. Chem.*, 2011, **3**, 157-159.
28. J.-Y. Ye and C.-J. Liu, *Chem. Commun.*, 2011, **47**, 2167-2169.
29. B. Xiao, P. S. Wheatley, X. Zhao, A. J. Fletcher, S. Fox, A. G. Rossi, I. L. Megson, S. Bordiga, L. Regli, K. M. Thomas and R. E. Morris, *J. Am. Chem. Soc.*, 2007, **129**, 1203-1209.
30. S. P. Petkov, G. N. Vayssilov, J. Liu, O. Shekhah, Y. Wang, C. Wöll and T. Heine, *Chem. Phys. Chem.*, 2012, **13**, 2025-2029.
31. J. Szanyi, M. Daturi, G. Clet, D. R. Baer and C. H. F. Peden, *Phys. Chem. Chem. Phys.*, 2012, **14**, 4383-4390.
32. J. Yang, T. Regier, J. J. Dynes, J. Wang, J. Shi, D. Peak, Y. Zhao, T. Hu, Y. Chen and J. S. Tse, *Anal. Chem.*, 2011, **83**, 7856-7862.
33. N. Nijem, P. Canepa, L. Kong, H. Wu, J. Li, T. Thonhauser and Y. J. Chabal, *J. Phys.: Condens. Matter*, 2012, **24**, 424203.
34. N. Nijem, L. Kong, Y. Zhao, H. Wu, J. Li, D. C. Langreth and Y. J. Chabal, *J. Am. Chem. Soc.*, 2011, **133**, 4782-4784.
35. N. Nijem, P. Thissen, Y. Yao, R. C. Longo, K. Roodenko, H. Wu, Y. Zhao, K. Cho, J. Li, D. C. Langreth and Y. J. Chabal, *J. Am. Chem. Soc.*, 2011, **133**, 12849-12857.
36. N. Nijem, J.-F. Veyan, L. Kong, K. Li, S. Pramanik, Y. Zhao, J. Li, D. Langreth and Y. J. Chabal, *J. Am. Chem. Soc.*, 2010, **132**, 1654-1664.
37. N. Nijem, J.-F. Veyan, L. Kong, H. Wu, Y. Zhao, J. Li, D. C. Langreth and Y. J. Chabal, *J. Am. Chem. Soc.*, 2010, **132**, 14834-14848.
38. N. Nijem, H. Wu, P. Canepa, A. Marti, K. J. Balkus, T. Thonhauser, J. Li and Y. J. Chabal, *J. Am. Chem. Soc.*, 2012, **134**, 15201-15204.
39. S. M. Chavan, O. Zavorotynska, C. Lamberti and S. Bordiga, *Dalt. Trans.*, 2013, **42**, 12586-12595.
40. V. Stavila, J. Volponi, A. M. Katzenmeyer, M. C. Dixon and M. D. Allendorf, *Chem. Sci.*, 2012, **3**, 1531-1540.
41. C. Munuera, O. Shekhah, H. Wang, C. Wöll and C. Ocal, *Phys. Chem. Chem. Phys.*, 2008, **10**, 7257-7261.
42. M. D. Allendorf, A. Schwartzberg, V. Stavila and A. A. Talin, *Chem. Eur. J.*, 2011, **17**, 11372-11388.
43. D. Zacher, K. Yusenko, A. Bétard, S. Henke, M. Molon, T. Ladnorg, O. Shekhah, B. Schüpbach, T. de los Arcos, M. Krasnopolski, M. Meilikhov, J. Winter, A. Terfort, C. Wöll and R. A. Fischer, *Chem. Eur. J.*, 2011, **17**, 1448-1455.
44. O. Shekhah, *Materials*, 2010, **3**, 1302-1315.
45. J. Baltrusaitis, P. M. Jayaweera and V. H. Grassian, *Phys. Chem. Chem. Phys.*, 2009, **11**, 8295-8305.
46. C. C. Chusuei and D. W. Goodman, *Encyclopedia of Physical Science and Technology*, 3 edn., R. A. Meyers, ed. Academic Press, NY, 2002.
47. M. Le, M. Ren, Z. Zhang, P. T. Sprunger, R. L. Kurtz and J. C. Flake, *J. Electrochem. Soc.*, 2011, **158**, E45-E49.
48. B. R. Strohmeier, D. E. Levden, R. S. Field and D. M. Hercules, *J. Catal.*, 1985, **94**, 514-530.
49. M. Radoń, P. Kozyra, A. Stępniewski, J. Datka and E. Broclawik, *Can. J. Chem.*, 2013, **91**, 538-543.

Table of Content

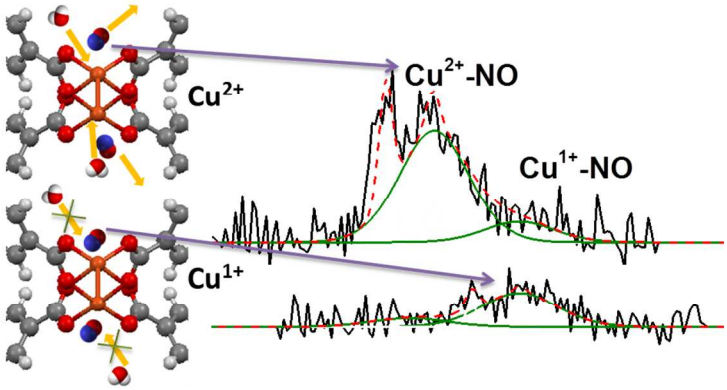

Photo-reduced Cu^{2+} in HKUST-1 adsorbs NO over water, underscoring the potential of MOFs with mixed oxidation metals for gas separation.